Wave Polarisation and Stokes Parameters

1 Wave Polarisation

Electromagnetic waves are transverse, meaning that their oscillations are perpendicular to their direction of propagation. If the wave vector and wave electric field define a plane that does not change as the wave propagates, then the wave is *linearly polarised*, since the wave is seen to define a line when viewed along the direction of propagation (as illustrated in figure 1). Characterizing the polarisation of an arbitrarily polarised, band limited wave is the subject of this section (see also Kraus 1986; Rohlfs and Wilson 2000).

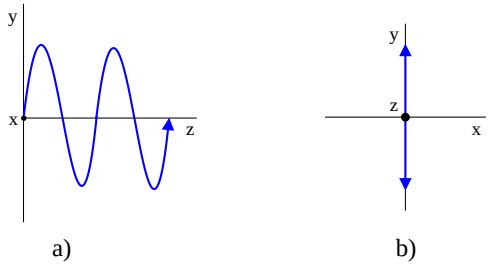

Figure 1: A linearly polarised wave in the y direction (y-z plane) viewed: a) parallel to the x axis, b) along the z axis, the direction of propagation.

1.1 The Polarisation Ellipse

Consider two orthogonal, linearly polarised electromagnetic waves of the same frequency travelling in the $\hat{\mathbf{k}}$ (z) direction, the first polarised in the x direction (x-z plane), the second in the y direction (y-z plane). The electric fields of the two waves, as illustrated in figure 2a, may be described by the following equations:

$$E_x = E_1 \cos(kz - \omega t) \quad (1)$$

$$E_y = E_2 \cos(kz - \omega t - \delta) \quad (2)$$

where k is the wavenumber, ω is the frequency, t is time, and δ is the phase offset between the two waves ($\delta = \delta_x - \delta_y$). The detected wave will be the vector sum of these two individual waves as illustrated in figure 2b and c. At $z = 0$, the components of $\mathbf{E}$ may be reduced to:

$$E_x = E_1 \cos(\omega t) \quad (3)$$

$$E_y = E_2 \cos(\omega t + \delta) \quad (4)$$

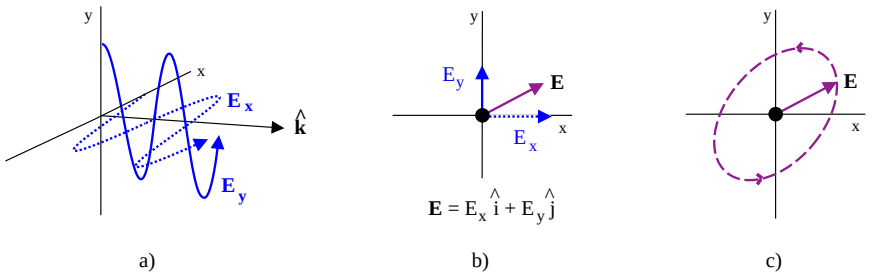

Figure 2: Wave Polarisation: a) Two orthogonal linearly polarised waves travelling in the z direction, b) addition of components, c) the locus of points of the tip of **E**.

Combining equation 3 and equation 4 results in the equation of an ellipse:

$$1 = aE_x{}^2 - bE_xE_y + cE_y{}^2 \tag{5}$$

where

$$a = \frac{1}{E_1{}^2\sin^2\delta} \qquad b = \frac{2\cos\delta}{E_1E_2\sin^2\delta} \qquad c = \frac{1}{E_2{}^2\sin^2\delta} \tag{6}$$

This equation describes the locus of points traced out by the vector **E** as the wave propagates through space. The ellipse, known as the polarisation ellipse, may be characterized by two angles, τ and ε, as illustrated in figure 3.

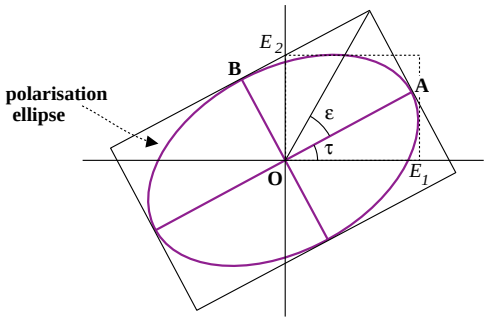

Figure 3: The Polarisation Ellipse (after figure 4.5 in Kraus 1986).

The angle τ is known as the tilt angle or polarisation angle. It gives a measure of inclination of the ellipse with respect to the x axis and is defined within the limits of $0° \leq \tau \leq 180°$. The second angle, ε, is determined by the ratio of the major axis (OA) to the minor axis (OB) through the relation:

$$\varepsilon = \cot^{-1}(\mp\frac{\mathrm{OA}}{\mathrm{OB}}) \tag{7}$$

and is defined within the limits $-45^\circ \leq \varepsilon \leq +45^\circ$. The use of the $\mp$ depends on the "handedness" of the wave. If **E** moves counterclockwise when viewed travelling towards the observer, as in figure 2c, then the wave is said to have "right-hand" polarisation and the negative sign is used. Conversely, if **E** moves clockwise as viewed from the same vantage point, the wave is said to have "left-hand" polarisation and the positive sign is used. This definition of handedness is the IEEE convention, and is the standard in radio astronomy, since it is consistent with the well known 'right hand rule'.[1]

Depending on the properties of E_1, E_2 and δ, the polarisation ellipse will take on different forms. In general, waves with $0^\circ < \delta < 180^\circ$ will be left elliptically polarised whereas waves with $180^\circ < \delta < 360^\circ$ ($-180^\circ < \delta < 0^\circ$) will be right elliptically polarised. If $\delta = 0^\circ$ or $\delta = 180^\circ$, the wave will be linearly polarised. In all of these cases, the polarisation angle of the wave subsequently depends on the relative amplitudes of E_1 and E_2. For example, if $E_1 = E_2$ and $\delta = 0$, the polarisation angle is 45° (note that $\varepsilon = 0$ in this case). Furthermore, if $E_1 = E_2$ and $\delta = 90^\circ$ [$\delta = 270^\circ$] the wave will be left [right] *circularly* polarised and τ is undefined. In cases where E_1, E_2 and δ are such that elliptical polarisation results, the wave can be thought of as having some component of linear polarisation, and some component of circular polarisation.

1.2 Stokes Parameters and the Poincaré Sphere

The state of polarisation represented by the polarisation ellipse may be described mathematically by the four so-called the Stokes parameters. Introduced by Stokes in 1852, they are

$$I = E_1^2 + E_2^2 \tag{8}$$

$$Q = E_1^2 - E_2^2 = I\cos 2\varepsilon \cos 2\tau \tag{9}$$

$$U = 2E_1E_2\cos\delta = I\cos 2\varepsilon \sin 2\tau \tag{10}$$

$$V = 2E_1E_2\sin\delta = I\sin 2\varepsilon \tag{11}$$

Stokes I is the total intensity of the wave, Stokes Q and U are measures of the linear polarisation of the wave, and Stokes V is a measure of the circular polarisation of the wave.

In this formalism of the Stokes parameters, I have used a linearly polarised basis. Alternatively, I could use a circularly polarised basis, since it

[1] Under the classical physics convention, the handedness definition is reversed. I use the IEEE convention.

is possible to construct a linearly polarised wave from two orthogonal circularly polarised waves. In this case, the definitions have the same form, except E_1 is replaced by E_r, the right circularly polarised amplitude, and E_2 is replaced by E_l, the left circularly polarised amplitude (Jackson, 1975). As I find it easier to visualize linearly polarised waves, I will continue my discussion using the linearly polarised basis.

Of the four parameters, only three are independent, since $I^2 = Q^2 + U^2 + V^2$. Since the Stokes parameters may be obtained from the observable quantities E_1, E_2, and δ, it is then possible to determine the polarisation angle of the wave from the relation

$$\tau = \frac{1}{2} \tan^{-1} \frac{U}{Q} \tag{12}$$

The Stokes parameters, when written in terms of τ and ε, are the Cartesian coordinates of the points on a sphere. This sphere is known as the Poincaré Sphere and provides an alternative way of describing the polarisation state of a wave. Figure 4a illustrates the sphere. For any location on the sphere, the longitude is given by 2τ, and the latitude by 2ε. The equator represents states of pure linear polarisation, while the poles represent states of pure circular polarisation. The northern hemisphere represents waves with left circular polarisation, while the southern hemisphere represents waves with right circular polarisation. Figure 4b shows one state of polarisation. From its location on the sphere, we know that the represented wave is left circularly polarised, with $2\tau \sim 45°$, and $2\varepsilon \sim 45°$. In addition Cartesian coordinates x and y, given by the Stokes parameters Q and U, indicate the type of linear polarisation of the wave, while the z coordinate, Stokes V, indicates the amount of circular polarisation.

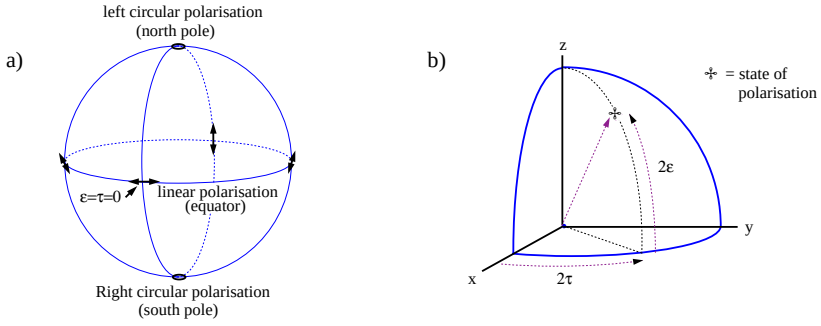

Figure 4: The Poincaré Sphere: a) The full sphere; b) One octant illustrating a state of polarisation (after figures 4.7 and 4.6 in Kraus 1986).

1.3 Time Variations and Partial Polarisation

The above discussion dealt with a completely polarised or monochromatic wave, where E_1, E_2 and δ are constant. In general, emissions from celestial radio sources usually extend over a wide range of frequencies. Within any finite range of frequencies detected by a receiver, the wave will consist of a superposition of a large number of statistically independent waves with a variety of polarisations. Thus equations 3 and 4 become

$$E_x = \sum_k E_k^{(1)} \cos(w_k t) = E_1(t)\cos(\omega t) \quad (13)$$

$$E_y = \sum_k E_k^{(2)} \cos(w_k t + \delta_k) = E_2(t)\cos(\omega t + \delta(t)) \quad (14)$$

where ω is now the mean frequency, and $E_1(t)$ and $E_2(t)$ are the time dependent amplitudes resulting from the addition of all independent E_1's and E_2's respectively. Due to the time dependence, it is necessary to take the time averages of the Stokes parameters, so that

$$I = < E_1^2 > + < E_2^2 > = S \quad (15)$$

$$Q = < E_1^2 > - < E_2^2 > = S < \cos 2\varepsilon \cos 2\tau > \quad (16)$$

$$U = 2 < E_1 E_2 \cos\delta > = S < \cos 2\varepsilon \sin 2\tau > \quad (17)$$

$$V = 2 < E_1 E_2 \sin\delta > = S < \sin 2\varepsilon > \quad (18)$$

As a result, it is now possible to have $I^2 \geq Q^2 + U^2 + V^2$. For a completely unpolarised wave, $Q = U = V = 0$. Thus the presence of a polarised component in the wave requires at least one of these components to be non-zero. The degree or fraction of polarisation is defined as

$$d_p = \frac{\text{polarised power}}{\text{total power}} = \frac{\sqrt{Q^2 + U^2 + V^2}}{S} \quad (19)$$

where $0 \leq d_p \leq 1$. Thus, $d_p = 1$ for a completely polarised wave, while $d = 0$ for a completely unpolarised wave. Similarly, the fraction of linear polarisation is defined as

$$M = \frac{\sqrt{Q^2 + U^2}}{S} \, . \quad (20)$$

2 Faraday Rotation

When a linearly polarised electromagnetic wave propagates through a region of magnetized plasma, its plane of polarisation will rotate, as illustrated in

figure 5 . This phenomenon is known as Faraday rotation. Faraday rotation can be understood as a consequence of *birefringence*, where the magnetised plasma has two different indices of refraction corresponding to two different states of incident polarisation (Hecht, 1998).

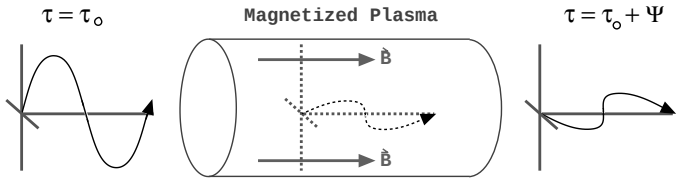

Figure 5: Faraday rotation of a polarised electromagnetic wave as it propagates through a magnetized plasma cloud.

In particular, the birefringence is with respect to right and left circularly polarised waves. Since a linearly polarised wave can be constructed from two circularly polarised waves, the birefringence will slow one of the circularly polarised waves with respect to the other, resulting in a rotation of their sum, the linearly polarised wave, as illustrated in figure 6.

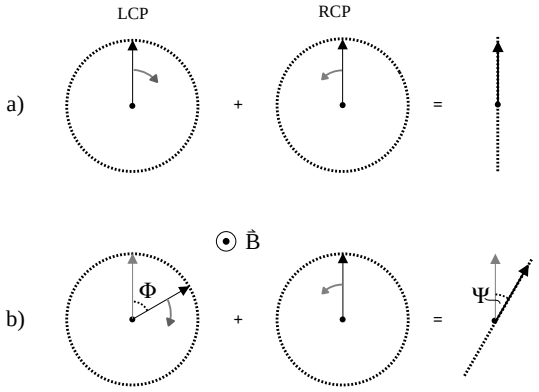

Figure 6: Faraday rotation through birefringence: a) linearly polarised wave decomposed into a left and right circularly polarised wave, b) the same wave after travelling through a birefringent medium. The LCP wave leads the RCP wave by a phase angle of Φ, resulting in a rotation of the linearly polarised wave by an angle Ψ (after figures 4.43 and 4.44 in Chen 1984).

To calculate the indices of refraction for a cosmic magnetised plasma,

the *quasi-longitudinal* (QL) approximation is invoked (Ratcliffe, 1962). The validity of the QL approximation depends on how closely the direction of propagation of a wave ($\hat{\mathbf{k}}$) coincides with the field direction ($\hat{\mathbf{b}}$), defined $\theta = \cos^{-1}(\hat{\mathbf{b}} \cdot \hat{\mathbf{k}})$, and on the electron density and the collision frequency. In practice, it is possible that the QL approximation is valid for values of θ deviating significantly from zero. As θ approaches 90°, a linearly polarised wave will aquire some ellipticity (known as the Cotton-Mouton effect), instead of simply rotating as it would in the QL regime.

The QL approximation is valid if (Hutchinson, 1987)

$$\frac{\Omega}{\omega} \sec\theta \ll 1 \tag{21}$$

and if

$$\frac{\omega_p^2}{\omega^2} \ll 1 \,, \tag{22}$$

where Ω is the cyclotron frequency, and ω_p is the plasma frequency. If the total strength of the Galactic magnetic field is, on average, roughly $B_\circ = 10\ \mu$G (10^{-9} T), the electron cyclotron frequency is

$$\begin{aligned} \Omega &= \frac{eB_\circ}{m_e} \\ &= 175.63 \quad \text{rad/s} \end{aligned} \tag{23}$$

where e and m_e are the electron charge and mass, respectively. If we set $(\Omega/\omega)\sec\theta = \frac{1}{1000}$, then with $\omega = 2\pi \times 1420$ MHz, the QL approximation holds for $\theta < 89.99887°$. Similarly, for equation 22, using $n_e = 1$ cm^{-3} (10^6 m^{-3}), the plasma frequency is

$$\begin{aligned} \omega_p &= \left(\frac{n_e e^2}{\epsilon_\circ m_e}\right)^{\frac{1}{2}} \\ &= 56 \times 10^3 \quad \text{rad/s} \end{aligned} \tag{24}$$

As a result, $\omega_p^2/\omega^2 = 4 \times 10^{-11} \ll 1$. Clearly, for radio wave propagation in the ISM, the QL approximation holds.

Using the QL approximation, the indices of refraction for circularly polarised waves in a magnetised plasma are (Spitzer, Jr., 1978)

$$N_\pm = \frac{c}{v} = \left[1 - \frac{{\omega_p}^2}{\omega^2}\left(1 \pm \frac{\Omega}{\omega}\cos\theta\right)^{-1}\right]^{\frac{1}{2}} \tag{25}$$

The '−' sign corresponds to the circular polarisation mode rotating in the same direction as an electron gyrating around the magnetic field line. In figure 6, the '−' sign would apply to the right circularly polarised wave. Conversely, the '+' sign refers to the circular polarisation mode rotating in the opposite direction of the electron gyration motion.

The phase difference, $\delta\Phi$, between the two circularly polarised waves travelling a distance dl through the medium is given by[2]

$$\delta\Phi \equiv (N_+ - N_-)\frac{\omega}{c}dl. \tag{26}$$

The linearly polarised wave subsequently rotates through an angle $d\Psi$:

$$d\Psi = \frac{\delta\Phi}{2}. \tag{27}$$

In order to calculate Ψ, the first task is to evaluate N_+ and N_-. To begin, let

$$\mathrm{A} = \frac{\omega_\mathrm{p}^2}{\omega^2}\left(1 + \frac{\Omega}{\omega}\cos\theta\right)^{-1} \tag{28}$$

and

$$\mathrm{B} = \frac{\omega_\mathrm{p}^2}{\omega^2}\left(1 - \frac{\Omega}{\omega}\cos\theta\right)^{-1} \tag{29}$$

Since $\omega_p^2/\omega^2 \ll 1$, then A and B are both much less than 1. Therefore, we can use the binomial approximation so that

$$N_+ \simeq 1 - \frac{1}{2}\mathrm{A} \tag{30}$$

and

$$N_- \simeq 1 - \frac{1}{2}\mathrm{B}. \tag{31}$$

Therefore,

$$\begin{aligned}\delta\Phi &\simeq \frac{1}{2}(\mathrm{B} - \mathrm{A})\frac{\omega}{c}dl \\ &\simeq \frac{1}{2}\frac{\omega_p^2}{\omega^2}\left[\left(1 - \frac{\Omega}{\omega}\cos\theta\right)^{-1} - \left(1 + \frac{\Omega}{\omega}\cos\theta\right)^{-1}\right].\end{aligned} \tag{32}$$

[2]I remind the reader that throughout this paper, dl is a differential path element *towards* the observer.

Since $\Omega/\omega \ll 1$, we can again use the binomial approximation to reduce this to

$$\begin{aligned} \delta\Phi &\simeq \frac{1}{2}\frac{\omega_p^2}{\omega^2}\left[1+\frac{\Omega}{\omega}\cos\theta - 1 + \frac{\Omega}{\omega}\cos\theta\right]\frac{\omega}{c}dl \\ &\simeq \frac{\omega_p^2}{\omega^2}\frac{\Omega}{c}\cos\theta dl. \end{aligned} \tag{33}$$

Substituting equation 33 into equation 27, and using equations 23 and 24, we find

$$d\Psi \simeq \frac{1}{2}\frac{e^3}{\epsilon_\circ m_e^2 c}\frac{1}{\omega}n_e B_\circ \cos\theta dl. \tag{34}$$

Replacing ω with $2\pi c/\lambda$, recognizing that $B_\circ \cos\theta dl = \mathbf{B}\cdot d\mathbf{l}$, and integrating over the full path length, gives

$$\Psi \simeq \lambda^2\left[\frac{e^3}{8\pi^2\epsilon_\circ {m_e}^2 c^3}\right]\int n_e \mathbf{B}\cdot d\mathbf{l}. \tag{35}$$

Substituting in the appropriate values yields

$$\Psi \simeq \lambda^2 2.631\times 10^{-13}\int n_e\mathbf{B}\cdot d\mathbf{l}\ \ (\text{rad}) \tag{36}$$

where the remaining variables are in mks units. In astronomy, however, it is more common to use cgs units. In addition, it is more practical to work with the magnetic field in units of μG, and path lengths in units of pc. Thus, multiplying equation 36 by the appropriate 'correction' factors (ie. 1 μG = 10^{-10} T, 1 pc = 3.085×10^{16} m, 1 cm = 0.01 m) yields

$$\begin{aligned} \Psi &\simeq \lambda^2(0.812\int n_e\mathbf{B}\cdot d\mathbf{l})\ \ (\text{rad}) \\ &\simeq \lambda^2 \text{RM} \end{aligned} \tag{37}$$

where λ is in units of m, n_e is in units of cm^{-3}, $\mathbf{B}$ is in units of μG, $d\mathbf{l}$ is in units of pc, and RM is the **rotation measure**:

$$\text{RM} = 0.812\int n_e\mathbf{B}\cdot d\mathbf{l}\ \ (\text{rad m}^{-2}). \tag{38}$$

It is important to recognize the significance of three key elements of equation 37. First, it is wavelength dependent. As a result, waves of different frequency will experience different amounts of rotation through the same plasma. Second, the effect of Faraday rotation is weighted by the electron

density; higher electron densities will result in greater rotation. Finally, it is the *direction* of the line-of-sight component of the magnetic field ($B_\parallel$) that determines the *sign* of the rotation measure. Since the path length is defined to be *from* the source *to* the receiver, (ie. the telescope on Earth), a magnetic field with $B_\parallel$ directed towards us results in a positive RM, while a magnetic field with $B_\parallel$ directed away from us results in a negative RM. It is this sign dependence that makes the rotation measure an extremely valuable tool for studying the magnetic field in the Galaxy.

3 Rotation Measure Sources

Two classes of astronomical object are used as sources for RM studies of the Galactic magnetic field. These are pulsars (within the Galaxy) and extragalactic sources, the latter including both external galaxies and quasars. These sources have been used in studies to explore the Galactic magnetic field.

Polarised emissions from the RM sources arise from *synchrotron radiation*. Synchrotron radiation is produced by relativistic electrons gyrating in a magnetic field (recall that accelerating charges *radiate*) The relativistic speeds of the electrons results in a 'beaming' of their radiation, much like a locomotive's headlight (Griffiths, 1999). The resulting radiation is primarily linearly polarised.[3] A source emitting synchrotron radiation can at most appear to have $d_p = 0.7$ (Pacholczyk, 1970). Any disordering of the magnetic field or the presence of Faraday rotation within the source will decrease the degree of polarisation.

Taylor et al. (1993) compiled a list of all known pulsars and their parameters, and maintain a publicly accessible database as more pulsars are discovered (Taylor et al., 1995). From this database (as it was in 1999), I constructed a list of pulsars with known rotation measures and combined it with a recently published list of another 63 pulsars (Han et al., 1999). In total, there are approximately 316 pulsars with known rotation measures. Figure 7 is an all-sky plot of RM for these pulsars. As shown, more than half (191) reside at low latitudes ($-8^\circ < b < 8^\circ$). Of these, only 38 are located in the outer Galaxy ($90^\circ < l < 270^\circ$).

Simard-Normandin et al. (1981) published an extensive all-sky catalog of 555 extragalactic RM sources. This catalog was combined with several smaller studies by Broten et al. (1988), who applied further selection criteria

[3]Observationally, extragalactic sources exhibit less than 0.5% fraction of circular polarisation (Roberts et al., 1975).

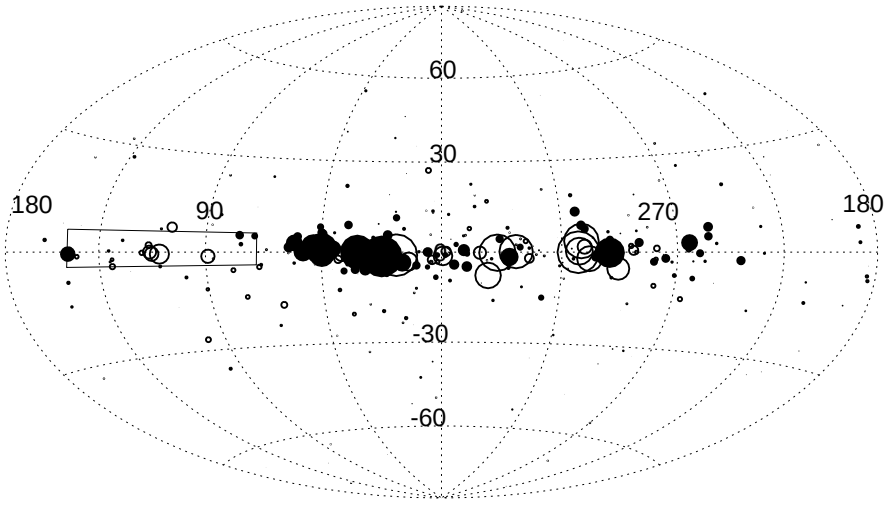

Figure 7: All-sky projection of pulsars with known rotation measures. Symbols are scaled with the magnitude of rotation measure to a maximum of 700 rad m^{-2}. Filled circles indicate positive RM; open circles indicate negative RM. The box indicates the Canadian Galactic Plane Survey (CGPS) region.

for Faraday-thin[4], one component sources, resulting in an enhanced catalog of 674 extragalactic RM sources. Since then, Clegg et al. (1992) determined the RM of 33 sources (some with mulitiple components) in the Galactic disk, while Oren and Wolfe (1995) and Minter and Spangler (1996) determined RMs for 61 and 38 high latitude sources, respectively. For my thesis, I consolidated the last four lists into one list of about 800 RM sources. Figure 8 is an all-sky plot of these sources. As illustrated, the sources are distributed somewhat uniformly, with an average source density of roughly 1 source per 80 square degrees. Of these, only 121 sources are located close to the Galactic disk ($-8^\circ < b < 8^\circ$) with only 53 having lines-of-sight primarily through the outer Galaxy ($90^\circ < l < 270^\circ$).

For my thesis work, I examined more than 700 polarised sources in the Canadian Galactic Plane Survey (CGPS). Using a detailed algorithm to

[4]Faraday-thin objects are small in the sense that waves emitted at the far end of the object do not undergo significant rotation by the time they reach the near end of the object. In other words, the emitted synchrotron radiation is in the *optically-thin* frequency range, and the object does not exhibit signs of any significant internal Faraday rotation. For a given object, the Faraday-thin regime is identified as the frequencies where the polarisation angle changes *linearly* with the square of the wavelength (Vallée, 1980).

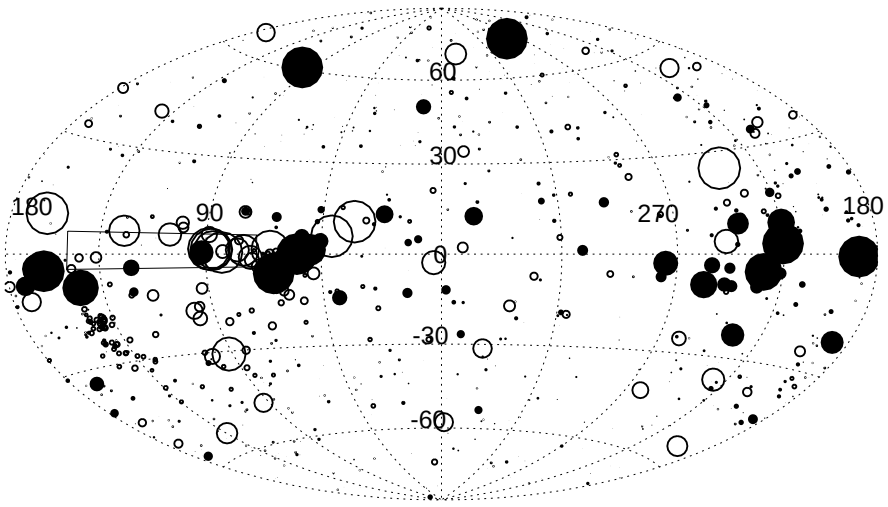

Figure 8: All-sky projection of extragalactic sources with known rotation measures. Symbols are scaled with the magnitude of rotation measure to a maxium of 700 rad m^{-2}. Filled circles indicate positive RM; open circles indicate negative RM. The box indicates the CGPS region.

sort through the data, verifying the quality of the rotation measures, these data were reduced to a list of 380 sources. Figure 9 is a plot of the RM sources in the CGPS region, before and after the addition of the new CGPS sources. This figure highlights the density of the CGPS sources, which is approximately 1 source per square degree.

The most striking qualitative feature of the data is the predominance of negative rotation measures throughout the CGPS region, and the systematic increase in |RM| with decreasing longitude. This result is consistent with the uniform magnetic field being approximately aligned with the spiral arms. At the higher longitudes in figure 9, we are looking almost perpendicular to our local arm, as well as to the Perseus and Outer arms. As a result, we would expect the line-of-sight component of the field to be small, producing low rotation measures. Conversely, at lower longitudes in figure 9, we are looking almost along our local arm, and therefore along the magnetic field lines. Since previous studies have demonstrated conclusively that the local field is directed away from us at $l \sim 90^\circ$, we would expect the magnitudes of the rotation measures at the lower longitudes to be large and negative, as demonstrated in this figure. In addition, the predominately negative values

indicate the average magnetic field in this region is directed away from us. These two insights provide important pieces in the puzzle to understand the global structure of the magnetic field in the Galaxy.

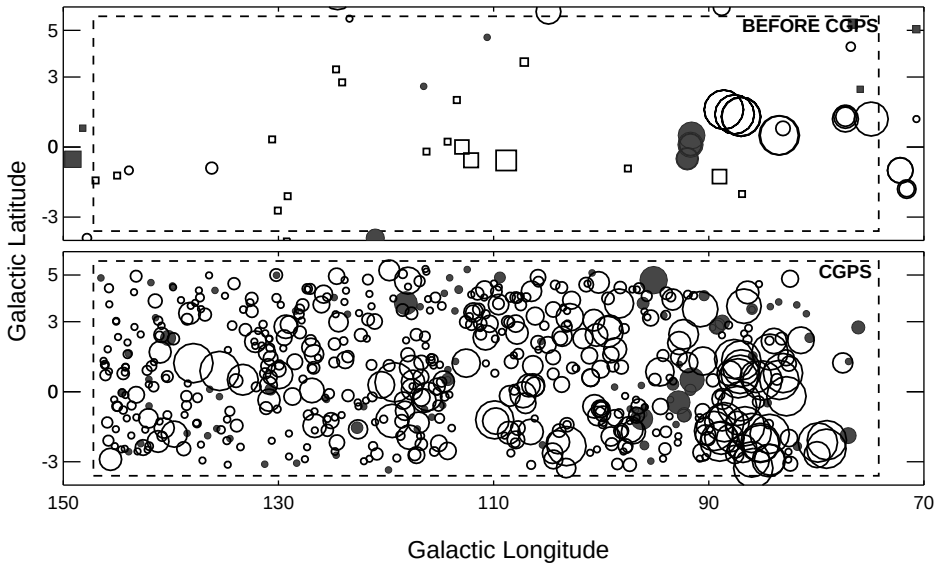

Figure 9: CGPS region (indicated by the dashed box) in rotation measure. Top panel: Previously observed EGS (circles) and pulsars (squares); Bottom panel: CGPS EGS sources. Source symbols are linearly scaled to the magnitude of the RM, between 100 and 600 rad m^{-2}. Filled circles are positive RM; open circles are negative RM.

References

Broten, N. W., MacLeod, J. M., and Vallée, J. P. 1988, *Astrophys. Space. Sci.*, 141, 303.

Chen, F. F. 1984, *Introduction to Plasma Physics and Controlled Fusion*, (Plenum Press).

Clegg, A. W., Cordes, J. M., Simonetti, J. M., and Kulkarni, S. R. 1992, *Astrophys. J.*, 386, 143.

Griffiths, D. J. 1999, *Introduction to Electrodynamics*, (Prentice-Hall, Inc.).

Han, J. L., Manchester, R. N., and Qiao, G. J. 1999, *Mon. Not. R. Astron. Soc.*, 306, 371.

Hecht, E. 1998, *Optics*, (Addison Wesley Longman Inc.).

Hutchinson, I. H. 1987, *Principles of Plasma Diagnostics*, (Cambridge Univ. Press).

Jackson, J. D. 1975, *Classical Electrodynamics*, (John Wiley & Sons Inc.).

Kraus, J. D. 1986, *Radio Astronomy*, (Cygnus-Quasar Books).

Minter, A. H. and Spangler, S. R. 1996, *Astrophys. J.*, 458, 194.

Oren, A. L. and Wolfe, A. M. 1995, *Astrophys. J.*, 445, 624.

Pacholczyk, A. G. 1970, *Radio Astrophysics*, (W.H. Freeman and Co.).

Ratcliffe, J. A. 1962, *The Magneto-Ionic Theory and Its Appliations to the Ionosphere*, (Cambridge Univ. Press).

Roberts, J. A., Cooke, D. J., Murray, J. D., Cooper, B. F. C., Roger, R. S., Ribes, J.-C., and Biraud, F. 1975, *Australian Journal of Physics*, 28, 325.

Rohlfs, K. and Wilson, T. L. 2000, *Tools of Radio Astronomy*, (Springer-Verlag), 3 edition.

Simard-Normandin, M., Kronberg, P. P., and Button, S. 1981, *Astrophys. J., Suppl. Ser.*, 45, 97.

Spitzer, Jr., L. 1978, *Physical Processes in the Interstellar Medium*, (John Wiley & Sons, Inc.).

Taylor, J. H., Manchester, R. N., and Lyne, A. G. 1993, *Astrophys. J., Suppl. Ser.*, 88, 529.

Taylor, J. H., Manchester, R. N., Lyne, A. G., and Camilo, F. 1995, *Catalog of 706 Pulsars*, http://pulsar.princeton.edu/pulsar.

Vallée, J. P. 1980, *Astron. Astrophys.*, 86, 251.